Proceedings of the 21st ICSMGE, Vienna, Austria, 14 – 19 June 2026. Pistrol, Adam & Schweiger (eds.)
Published by: ÖGG, Austrian Society for Geomechanics, Salzburg, Austria, ISBN 978-3-9503898-4-5
https://doi.org/10.53243/ICSMGE2026-706

Explainable artificial intelligence (XAI)-driven insights into the strength of cement-stabilized soils

Muhammad Hasnain Ayub Khan, Olivier Cuisinier, Adel Abdallah
Université de Lorraine, CNRS, LEMTA, F-54000 Nancy, France, muhammad-hasnain-ayu.khan@univ-lorraine.fr

ABSTRACT: Cement-soil stabilization is a widely practiced ground improvement technique, however, evaluating the strength development in cement-stabilized soils remains challenging due to the complex interplay of controlling factors such as compaction conditions, soil type, cement dosage and quality, curing time, etc. In the existing literature, while laboratory tests followed by empirical modeling to correlate the controlling factors with the unconfined compressive strength (UCS) are limited to specific soil-cement types, machine learning models often prioritize accuracy over interpretability. This study bridges the gap by considering diverse conditions pertaining to soil and cement types while evaluating strength development in cement-stabilized soils and employing explainable artificial intelligence to evaluate the relative importance and interactions of factors influencing UCS. A comprehensive database covering diverse soil and cement types was compiled from the literature, and a grid-search optimized extreme gradient boost (XGB) model was developed using features related to soil classification, compaction conditions, cement dosage and quality, curing time, and the porosity-to-volumetric cement content ratio. The model exhibited good generalization on an independently generated laboratory dataset. Using SHapley Additive Explanations (SHAP), the influence of individual features on the UCS was accessed. SHAP dependency analysis further uncovered significant interactions between features, particularly highlighting the critical role of compaction parameters as they interacted with most of the features. The SHAP analysis inspired the development of novel design charts, developed using an artificially generated dataset, offering optimal combinations of dry density and water content to achieve the desired UCS at fixed cement dosages.

KEYWORDS: Cement-stabilized soils, Explainable artificial intelligence, XGB, SHAP, Design charts

1 INTRODUCTION

Cement soil stabilization is widely practiced to enhance the mechanical properties of soils, particularly in pavement layers, rammed earth walls, embankments, earthen dams, and shallow foundations (Catton, 1962; Dupas and Pecker, 1979; Porbaha, Tanaka and Kobayashi, 1998; Jayasinghe and Kamaladasa, 2007; Tripura et al., 2020). It involves mixing cement, soil, and water, compacted to achieve the desired density. Strength development in cement-treated soils (CTS) is influenced by cement hydration, pozzolanic reactions, carbonation, and suction development. While short-term strength gain primarily comes from cement hydration, long-term strength is driven by the pozzolanic reaction between clay minerals and calcium hydroxide (Kézdi, 1979; Kitazume and Terashi, 2013). Carbonation also contributes to both short- (Chen et al., 2009) and long-term strength (Nakarai and Yoshida, 2015).

Several factors affect the efficiency of CTS, including soil properties (e.g., grain size, porosity, Atterberg limits), compaction conditions, binder quality, curing time, and curing conditions (Moore, Kennedy and Hudson, 1970; Porbaha, Tanaka and Kobayashi, 1998; Consoli, Rotta and Prietto, 2000; Sariosseiri and Muhunthan, 2009; Lepakshi and Reddy, 2020; Khan, Abdallah and Cuisinier, 2025). Though laboratory studies can assess the individual impact of these factors, their combined effects are more complex to evaluate. Empirical equations are proposed to account for the combined effect such factors.

For instance, (Lorenzo and Bergado, 2004) identified the post-curing void ratio to cement content ratio and cement content as crucial for strength in high-moisture CTS and presented an empirical equation correlating these factors with UCS. (Consoli et al., 2011) introduced the porosity/volumetric cement content ratio (η/C_{iv}) to explain the effects of porosity and cement dosage on UCS. (Horpibulsuk, Miura and Nagaraj, 2003; Tsuchida and Tang, 2015) developed predictive equations for UCS based on variables like water-cement ratio, volumetric solid content, and cement content. (Kang, Tsuchida and Athapaththu, 2015; 2016; Chian, Nguyen and Phoon, 2016) created empirical models accounting for factors like water-cement ratio, liquid limit, specific volume, and curing time. While empirical equations have provided a straightforward approach for predicting the UCS of CTS, their reliance on a limited set of parameters restricts their applicability across various soil and cement types. Moreover, the complex interactions and relative significance of these factors on UCS are not well understood, limiting the accuracy and versatility of these models.

To overcome these limitations, recent advancements in artificial intelligence (AI) have aimed to improve prediction accuracy. However, while AI models excel at making predictions, they often lack transparency, making it challenging to interpret the factors driving those predictions. This is where explainable AI (XAI) steps in, offering a solution that combines the predictive power of AI with transparency. By providing clear, interpretable results, XAI ensures that users can trust the model and gain deeper insights into the relationships between the input factors and UCS.

This research addresses the gap between empirical models and AI-driven predictions by developing an XAI-based model for predicting UCS in CTS. Using a diverse dataset collected from the literature, this study uses the extreme gradient boost (XGB) algorithm to predict UCS based on key factors such as liquid limit, fine contents, cement dosage and type, curing time, η/C_{iv}, and compaction parameters. To enhance the model's interpretability, the Shapley additive explanation (SHAP) method is employed. SHAP not only helps explain the model's predictions but also provides valuable insights into how each factor influences UCS.

The resulting XAI-based model not only offers accurate predictions but also provides valuable insights into the influence of individual factors, which are then utilized to develop design charts. These charts provide optimal combinations of compaction parameters, such as dry density and water content, to achieve the desired UCS at specific cement dosages. This and a separately build user-interface make the model a practical and user-friendly tool for real-world engineering applications, aiding in the efficient design of cement-stabilized soils.

.

2 METHODOLOGY

2.1 *Research framework*

The flow chart of the predictive modeling is shown in Figure 1.

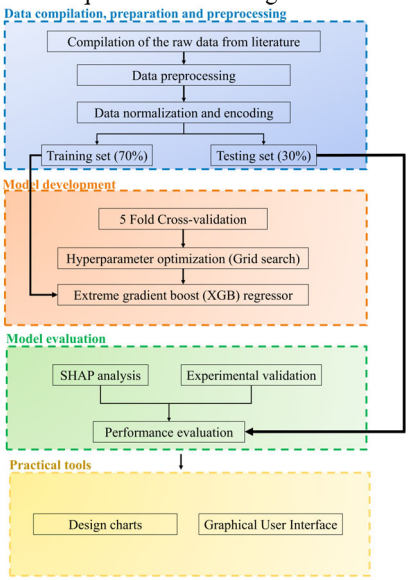

Figure 1. Flowchart of the methodology

2.2 *Data compilation*

To build a comprehensive CTS database across various soil and cement types, data from multiple literature sources were compiled (Abdallah, Russo and Cuisinier, 2023; Dong et al., 2022; Chamling, Biswal and Sahoo, 2021; Nguyen et al., 2020; Baldovino et al., 2020; Mengue et al., 2017; Beckett and Ciancio, 2014).The dataset includes four soil types: low plastic clay (CL), high plastic silt (MH), silty sand (SM), and poorly graded sand (SP), with CL making up the majority (120 records), followed by MH (92), SM (50), and SP (18). Fine-grained soils (clays and silts) account for 75% of the data, while coarse-grained soils (sands) make up 25%. Key features include liquid limit (LL), fine contents (FC), initial dry density normalized with respect to maximum dry density (ρ_{norm}), initial water content normalized with respect to optimum water content (ω_{norm}), cement dosage (C), curing time (T), porosity to volumetric cement content ratio (η/C_{iv}) as continuous variables and cement type (CEM-I, CEM-II, CEM-III) as categorical variable. One-hot encoding transformed the categorical cement type labels into binary format, where 1 denotes the presence and 0 the absence of a specific cement type. The descriptive statistics of the data is given in Table 1, where Min, Max and SD are the minimum, maximum and standard deviation values.

Table 1. Descriptive statistics of the data.

	Records	Min	Max	Mean	SD
LL	280	0	54	38.04	14.92
FC	280	1	99.2	70.9	29.5
ρ_{norm}	280	0.82	1.07	0.95	0.06
ω_{norm}	280	0.32	1.83	1.01	0.25
C	280	1	10	5.25	2.22
T	280	0	90	26.7	28.8
η/C_{iv}	280	5.77	78.2	16.4	10.3
UCS	280	38	5610	1736	1343.6

2.3 *Data pre-processing*

The Pearson's correlation plot in Figure 2 displays the Pearson's correlation coefficients (R), highlighting linear relationships between features. Notably, η/C_{iv} and FC show an inverse correlation with UCS, while ρ_{norm} is strongly and positively correlated. Although ω_{norm} has a weak direct correlation with UCS, its notable correlation with C suggests its relevance. Pearson's R also helps identify multicollinearity, where $|R| \geq 0.8$ typically indicates the presence of multicollinearity among the variables (Barton and Peat, 2014; Nawaz et al., 2024). The analysis confirms no multicollinearity among input features and shows all are sufficiently correlated with UCS for machine learning modeling.

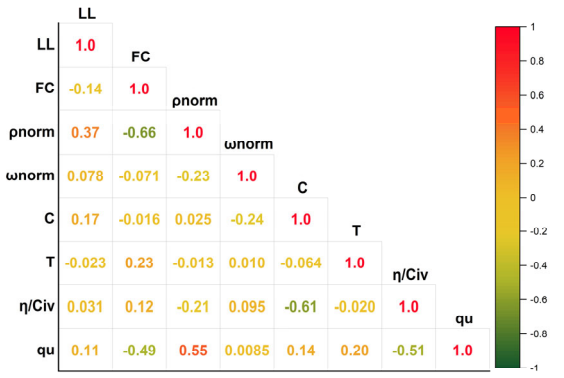

Figure 2. Scatter matrix plot of the data

Pearson correlation helps identify pairwise multicollinearity but falls short when multiple independent variables are involved. To address this, the Variance Inflation Factor (VIF) is used, as it measures how much a variable is correlated with all other independent variables. A VIF above 10 indicates high multicollinearity (Neter et al., 1996). As shown in Figure 3, all input features have VIF values well below 10, confirming the absence of multicollinearity.

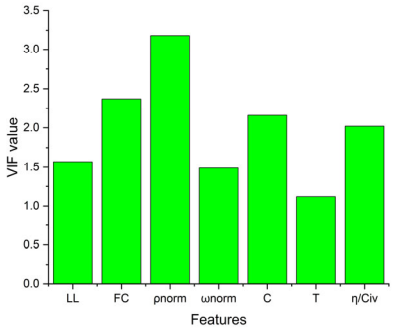

Figure 3. VIF value of the features

2.4 *Model development*

In this study, Extreme Gradient Boosting (XGB) is employed to predict the strength of CTS due to its robustness with smaller datasets and its ability to effectively mitigate overfitting through regularization techniques and early stopping (Gabriel and Anbarasi, 2023). XGB, developed by (Chen and Guestrin, 2016), is a powerful tree-based ensemble learning algorithm that builds upon the gradient boosting framework, offering improved efficiency, scalability, and model (Zhao et al., 2022). In XGB, decision trees, referred to as weak learners, are built sequentially, with each tree trained to minimize the residual errors of the previous one (Nguyen et al., 2023). The process begins with a base prediction, and subsequent trees iteratively correct the errors of prior models, as illustrated in Figure. 4. Unlike traditional gradient descent methods, XGB utilizes the Newton-Raphson optimization technique to more accurately estimate the optimal direction and step size for minimizing the

loss function. Additionally, XGB supports both L1 (Lasso) and L2 (Ridge) regularization to help prevent overfitting.

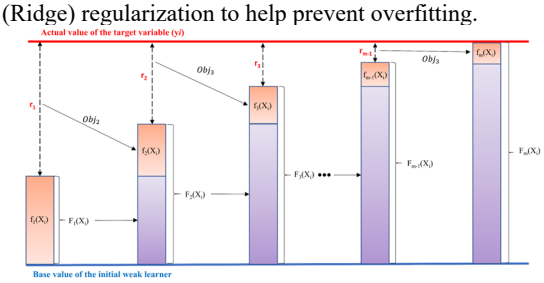

Figure. 4. Boosting in XGB algorithm (Potdar, Pardawala and Pai, 2017)

Complex models like tree-based algorithms are often considered black-box models due to their limited interpretability, necessitating the use of explanatory tools. The integration of such tools is known as Explainable Artificial Intelligence (XAI). In this study, SHAP (SHapley Additive exPlanations) was used to interpret the XGB model due to its theoretical grounding in game theory and its ability to attribute contributions to individual input features (Lundberg and Lee, 2017). SHAP calculates the contribution of each feature to a prediction by comparing outputs across different subsets of features. SHAP values offer insight into how much each feature drives the model's prediction away from the average output. For instance, in Figure. 5, three features contribute differently to the final prediction. Positive SHAP values (in red) increase the output, while negative values (in blue) decrease it. Larger absolute SHAP values indicate greater influence, regardless of direction.

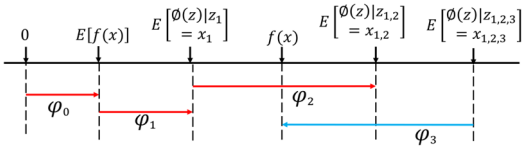

Figure. 5. Explanation of feature contribution through SHAP (Wang et al., 2023)

3 RESULTS

3.1 *Predictive performance of XGB model*

The UCS of CTS was predicted using the XGB algorithm with input features including liquid limit (LL), fine content (FC), normalized dry density (ρ_{norm}), normalized water content (ω_{norm}), cement dosage (C), curing time (T), porosity-to-volumetric cement ratio (η/C_{iv}), and cement types (CEM-I, II, III). XGB trains decision trees iteratively by minimizing a loss function using gradient and hessian updates. To enhance model performance, optimal hyperparameters were selected via grid search method. The dataset was randomly split into 70% training and 30% testing sets. The optimal hyperparameter values identified were: *max_depth = 5* (controls tree depth), *learning_rate = 0.2* (step size at each iteration to reduce loss), *n_estimators = 150* (number of trees to generate), *min_child_weight = 7* (minimum sum of observation weights in a child), *subsample = 0.8* (fraction of observations sampled for each tree), *colsample_bytree = 0.6* (fraction of features sampled for each tree), and *reg_lambda = 0.6* (penalizes loss function to prevent overfitting).

Figure 6 and Figure 7 present regression plots of actual versus predicted UCS values, including 90% prediction bands and error distribution plots for training and testing, respectively. Most data points closely follow the ideal fit line and fall within the prediction band, indicating strong model performance with high coefficient of determination (R^2) values (Khan et al., 2024). Error distribution plots show errors centered around zero, with mean errors of -0.67 kPa for training and -12.68 kPa for testing. The insets display absolute error trends across datasets. The average absolute error was 63.88 kPa for training and 152.08 kPa for testing, confirming the XGB model's high predictive accuracy.

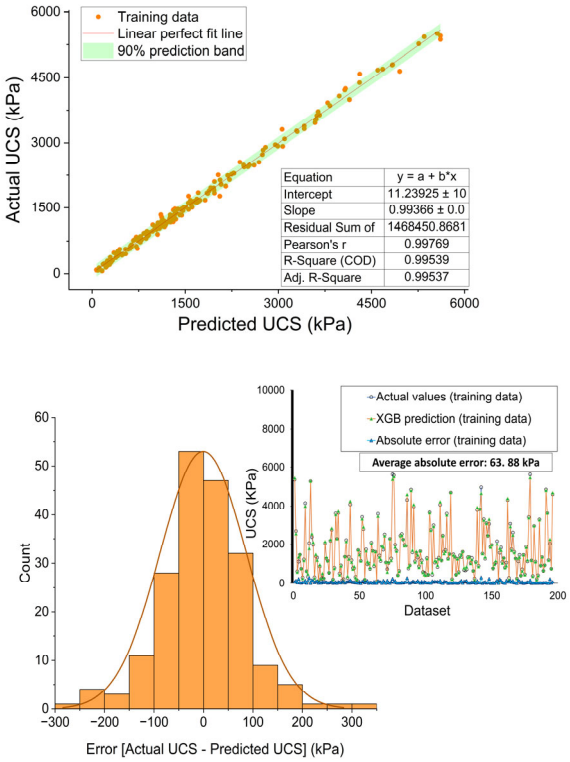

Figure 6. Regression and error distribution plots for the training set

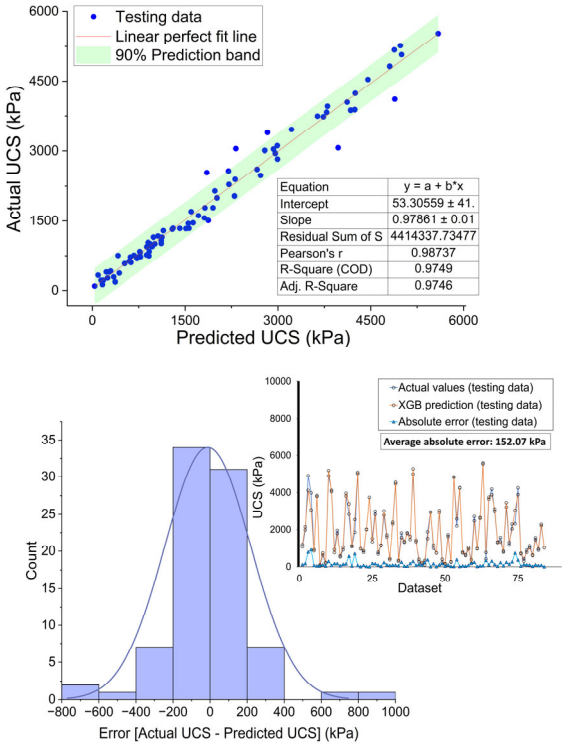

Figure 7. Regression and error distribution plots for the testing set

3.2 *Insights into the prediction via SHAP*

SHAP global interpretation provides insights into how each input feature generally impacts model predictions. It allows us to visualize both the relative importance and the average effect of each feature. Figure 8 presents the features used in model development ranked by their mean absolute SHAP values across the training data. Curing time (T) emerges as the most significant factor, with a mean SHAP value of 343.15 kPa, which is consistent with the XGB-based predictive modeling of UCS in stabilized soils reported in the literature (Chen, Hu and Wu, 2024). T is followed by η/C_{iv} (336.4 kPa), ρ_{norm} (267 kPa), ω_{norm} (232.18 kPa), and cement dosage (C). Among cement types, CEM-I shows a relatively high impact (109.5 kPa) compared to CEM-II (7.62 kPa) and CEM-III (2.49 kPa). Overall, cement type, LL, and FC have less influence compared to T, η/C_{iv}, C, ρ_{norm}, and ω_{norm}.

Figure 9 shows the SHAP summary plot for the optimized XGB model, where each dot represents an observation. Color indicates the feature value (blue for low, red for high), and position shows whether it contributes positively or negatively to UCS. The plot reveals that higher values of T, ρ_{norm}, C, and CEM-I positively affect UCS, while increases in η/C_{iv}, ω_{norm}, FC, and LL tend to reduce strength. SHAP thus not only identifies the most impactful features but also clarifies the nature of their relationship with UCS.

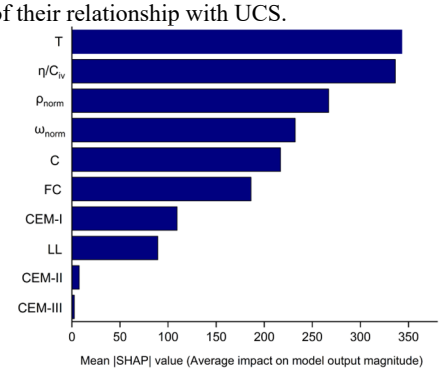

Figure 8. SHAP feature importance of XGB model

Figure 9. SHAP summary plot of XGB model

4 MODEL DEPLOYMENT AND USER ACCESSIBILITY

4.1 *Design charts*

SHAP analysis revealed that most input features interact with compaction parameters (ρ_{norm} and ω_{norm}), significantly influencing UCS predictions. This observation led to UCS optimization based on compaction parameters and inspired the creation of design charts. The data generation approach, illustrated in Fig. 16, was adapted from (Kardani et al., 2021) , who created engineered datasets to develop contour plots for unsaturated cemented soils.

To build the artificial dataset for design charts, various input combinations were used: cement content (C) at 3% and 6%; liquid limit (LL) at 0%, 30%, and 54%; fine content (FC) at 1%, 50%, and 99%; and ρ_{norm} and ω_{norm} values ranging from 0.9 to 1.1 in 0.05 increments as shown in Figure 10. Curing time (T) was fixed at 28 days. This generated 450 data points. Since η/C_{iv} can't be directly assumed, it was calculated using specific gravities of soil (2.7) and cement (3.11), and a soil maximum dry density of 17 kN/m³. The degree of saturation was also computed, leading to the removal of 54 invalid points with saturation >1, leaving 396 valid entries.

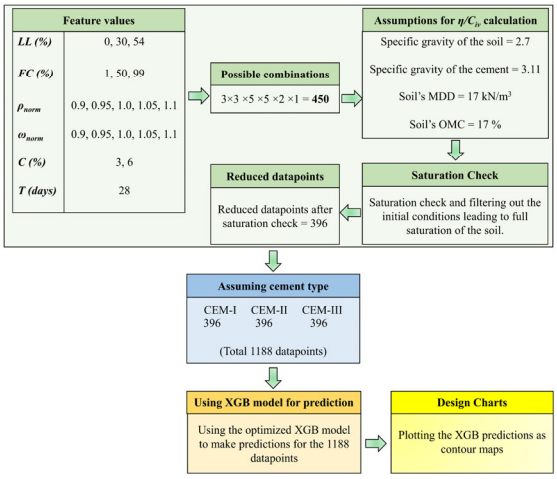

Figure 10. Conceptualization of developing design charts

The conventional mix design for cement-stabilized subgrade soils involves determining soil classification, cement type and dosage, compaction characteristics, and UCS through multiple tests. This dosage-based method identifies the optimum cement content by plotting UCS vs. cement dosage (Figure 11), typically accompanied by a moisture-density curve.

In contrast, the design charts developed in this study offer a more efficient alternative by optimizing strength through compaction parameters (Figure 12). These charts provide combinations of normalized dry density and water content needed to achieve a target UCS for specific cement types and dosages. For example, Figure 12 shows all ρ_{norm} and ω_{norm} combinations (highlighted by the red contour) that result in a UCS of 1600 kPa. This approach shifts focus from adjusting cement dosage to controlling compaction, which is often more economical. Moreover, unlike the traditional method, it eliminates the need for multiple UCS tests. Once the target strength is defined, the charts directly offer feasible compaction options to achieve it.

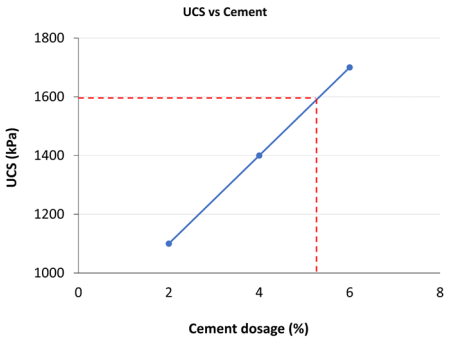

Figure 11. Traditional approach with 1600 kPa as the desired strength

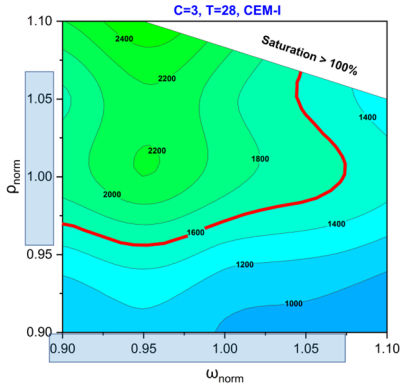

Figure 12. Possible combinations of dry density and water content to achieve the desired strength at fixed cement

4.2 *Graphical user interface*

A graphical user interface (GUI) was developed using Python's Streamlit library and is available on a GitHub repository (Figure 13). It provides a two-step UCS prediction process for CTS. In the first step, users input initial and maximum dry densities, initial and optimum water contents, specific gravities of soil and cement, and cement dosage. The interface then calculates η/C_{iv}, ρ_{norm}, and ω_{norm}, and checks for consistency by evaluating the degree of saturation and ensuring ρ_{norm} and ω_{norm} are within valid ranges.

If the inputs meet these criteria, the GUI proceeds to step two, where users enter the liquid limit, fine content, and cement type. As shown in Figure 14, clicking "Predict UCS" triggers strength predictions for curing times of 7, 14, and 28 days, with a visual display of strength progression over time. The interface can be accessed via the repository (Khan, Abdallah and Cuisinier, 2024).

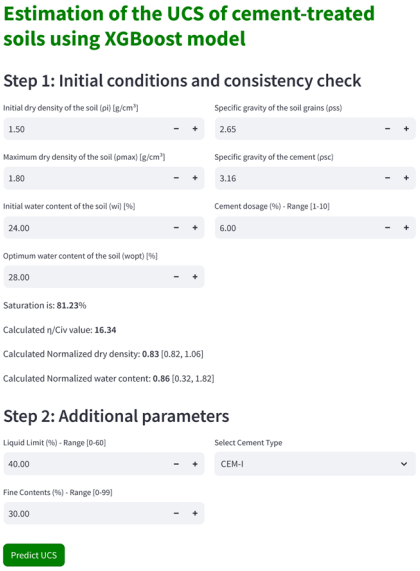

Figure 13. Graphical user interface for estimation of the UCS of CTS

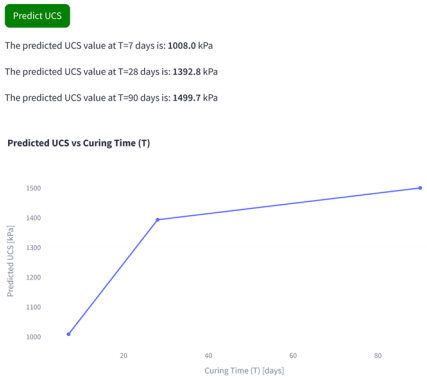

Figure 14. Prediction and visualization of the strength development with time

5 CONCLUSIONS

This study investigates strength development in CTS using XAI to assess and interpret the influence of key factors. The research led to a high-performing predictive model. The main findings are summarized below:

1. A comprehensive dataset of 280 records was compiled from the literature, covering various soil and cement types. Key input features included LL, FC, ρ_{norm}, ω_{norm}, C, T, η/C_{iv}, cement types, and UCS.
2. An XGB-based model was developed and optimized using grid search, achieving strong predictive performance with R^2 values of 0.99 (training) and 0.97 (testing).
3. SHAP analysis showed T, η/C_{iv}, ρ_{norm}, ω_{norm}, and C were the most influential features, while cement and soil types had lesser impact.
4. SHAP also revealed that while ρ_{norm}, ω_{norm} may rank lower individually, they interact significantly with other features.
5. Using an artificially generated dataset and the trained XGB model, UCS design charts were developed. These charts allow engineers to optimize strength by adjusting compaction parameters rather than cement dosage, offering a more cost-effective design method.
6. A user-friendly GUI, built with Streamlit, enables practitioners to use the XGB model without programming skills.

6 ACKNOWLEDGEMENTS

The study is funded by Agence Nationale de la Recherche (ANR), France, under the research project "Lorraine Artificial Intelligence (LORAI)" (project number: ANR-20-THIA-0010-01). The financial support is gratefully acknowledged.

7 REFERENCES

Abdallah, A., Russo, G. and Cuisinier, O., 2023. Statistical and Predictive Analyses of the Strength Development of a Cement-Treated Clayey Soil. *Geotechnics*, 3(2), pp.465–479.

Baldovino, J. de J.A., Izzo, R.L. dos S., Pereira, M.D., Rocha, E.V. de G., Rose, J.L. and Bordignon, V.R., 2020. Equations controlling tensile and compressive strength ratio of sedimentary soil–cement mixtures under optimal compaction conditions. *Journal of Materials in Civil Engineering*, 32(1), p.04019320.

Barton, B. and Peat, J., 2014. *Medical statistics: A guide to SPSS, data analysis and critical appraisal*. John Wiley & Sons.

Beckett, C. and Ciancio, D., 2014. Effect of compaction water content on the strength of cement-stabilized rammed earth materials. *Canadian geotechnical journal*, 51(5), pp.583–590.

Catton, M.D., 1962. Soil-Cement Technology-A Resume. *Portland Cement Assoc R & D Lab Bull*.

Chamling, P.K., Biswal, D.R. and Sahoo, U.C., 2021. Effect of moulding water content on strength characteristics of a cement-stabilized granular lateritic soil. *Innovative Infrastructure Solutions*, 6, pp.1–10.

Chen, Q., Hu, G. and Wu, J., 2024. Comparative study on the prediction of the unconfined compressive strength of the one-part geopolymer stabilized soil by using different hybrid machine learning models. *Case Studies in Construction Materials*, 21, p.e03439.

Chen, Q., Ke, Y., Zhang, L., Tyrer, M., Hills, C.D. and Xue, G., 2009. Application of accelerated carbonation with a combination of Na2CO3 and CO2 in cement-based solidification/stabilization of heavy metal-bearing sediment. *Journal of hazardous materials*, 166(1), pp.421–427.

Chen, T. and Guestrin, C., 2016. Xgboost: A scalable tree boosting system. Proceedings of the 22nd acm sigkdd international conference on knowledge discovery and data mining. pp.785–794.

Chian, S., Nguyen, S. and Phoon, K., 2016. Extended strength development model of cement-treated clay. *Journal of Geotechnical and Geoenvironmental Engineering*, 142(2), p.06015014.

Consoli, N., Rotta, G. and Prietto, P., 2000. Influence of curing under stress on the triaxial response of cemented soils. *Geotechnique*, 50(1), pp.99–105.

Consoli, N.C., Rosa, D.A., Cruz, R.C. and Dalla Rosa, A., 2011. Water content, porosity and cement content as parameters controlling strength of artificially cemented silty soil. *Engineering Geology*, 122(3–4), pp.328–333.

Dong, X., Bao, X., Cui, H., Xu, C. and Chen, X., 2022. Effects of cement treatment on mechanical properties and microstructure of a granite residual soil. *Applied Sciences*, 12(24), p.12549.

Dupas, J.-M. and Pecker, A., 1979. Static and dynamic properties of sand-cement. *Journal of the Geotechnical Engineering Division*, 105(3), pp.419–436.

Gabriel, J.J. and Anbarasi, L.J., 2023. Optimizing Coronary Artery Disease Diagnosis: A Heuristic Approach using Robust Data Preprocessing and Automated Hyperparameter Tuning of eXtreme Gradient Boosting. *IEEE Access*.

Horpibulsuk, S., Miura, N. and Nagaraj, T., 2003. Assessment of strength development in cement-admixed high water content clays with Abrams' law as a basis. *Geotechnique*, 53(4), pp.439–444.

Jayasinghe, C. and Kamaladasa, N., 2007. Compressive strength characteristics of cement stabilized rammed earth walls. *Construction and Building Materials*, 21(11), pp.1971–1976.

Kang, G., Tsuchida, T. and Athapaththu, A., 2015. Strength mobilization of cement-treated dredged clay during the early stages of curing. *Soils and Foundations*, 55(2), pp.375–392.

Kang, G., Tsuchida, T. and Athapaththu, A., 2016. Engineering behavior of cement-treated marine dredged clay during early and later stages of curing. *Engineering Geology*, 209, pp.163–174.

Kardani, N., Zhou, A., Shen, S.-L. and Nazem, M., 2021. Estimating unconfined compressive strength of unsaturated cemented soils using alternative evolutionary approaches. *Transportation Geotechnics*, 29, p.100591.

Kézdi, Á., 1979. *Stabilized earth roads*. Elsevier.

Khan, M.H.A., Abdallah, A. and Cuisinier, O., 2024. *Optimized XGB-based predictive modeling of the UCS of cement-treated soils*. https://doi.org/10.5281/zenodo.13890356.

Khan, M.H.A., Abdallah, A. and Cuisinier, O., 2025. Insights into the strength development in cement-treated soils: An explainable AI-based approach for optimized mix design. *Computers and Geotechnics*, 180, p.107103.

Khan, M.H.A., Jafri, T.H., Ud-Din, S., Ullah, H.S. and Nawaz, M.N., 2024. Prediction of soil compaction parameters through the development and experimental validation of Gaussian process regression models. *Environmental Earth Sciences*, 83(4), p.129.

Kitazume, M. and Terashi, M., 2013. *The deep mixing method*. CRC press London.

Lepakshi, R. and Reddy, B.V., 2020. Shear strength parameters and Mohr-Coulomb failure envelopes for cement stabilised rammed earth. *Construction and Building Materials*, 249, p.118708.

Lorenzo, G.A. and Bergado, D.T., 2004. Fundamental parameters of cement-admixed clay—New approach. *Journal of geotechnical and geoenvironmental engineering*, 130(10), pp.1042–1050.

Lundberg, S.M. and Lee, S.-I., 2017. A unified approach to interpreting model predictions. *Advances in neural information processing systems*, 30.

Mengue, E., Mroueh, H., Lancelot, L. and Eko, R.M., 2017. Mechanical improvement of a fine-grained lateritic soil treated with cement for use in road construction. *Journal of Materials in Civil Engineering*, 29(11), p.04017206.

Moore, R.K., Kennedy, T.W. and Hudson, W.R., 1970. Factors affecting the tensile strength of cement-treated materials. *Highway Research Record*, 315, pp.64–80.

Nakarai, K. and Yoshida, T., 2015. Effect of carbonation on strength development of cement-treated Toyoura silica sand. *Soils and Foundations*, 55(4), pp.857–865.

Nawaz, M.N., Akhtar, A.Y., Hassan, W., Khan, M.H.A. and Nawaz, M.M., 2024. Artificial intelligence-based prediction models of bio-treated sand strength for sustainable and green infrastructure applications. *Transportation Geotechnics*, 46, p.101262.

Neter, J., Kutner, M.H., Nachtsheim, C.J. and Wasserman, W., 1996. Applied linear statistical models.

Nguyen, M.-D., Le, A.-T., Nguyen, T.-A., Thach, N.-T. and Phan, T.-K., 2020. The Influence of Water Content and Compaction on the Unconfined Compression Strength of Cement Treated Clay. 2020 5th International Conference on Green Technology and Sustainable Development (GTSD). IEEE. pp.175–179.

Nguyen, T., Ly, D.-K., Huynh, T.Q. and Nguyen, T.T., 2023. Soft computing for determining base resistance of super-long piles in soft soil: A coupled SPBO-XGBoost approach. *Computers and Geotechnics*, 162, p.105707.

Porbaha, A., Tanaka, H. and Kobayashi, M., 1998. State of the art in deep mixing technology: part II. Applications. *Proceedings of the Institution of Civil Engineers-Ground Improvement*, 2(3), pp.125–139.

Potdar, K., Pardawala, T.S. and Pai, C.D., 2017. A comparative study of categorical variable encoding techniques for neural network classifiers. *International journal of computer applications*, 175(4), pp.7–9.

Sariosseiri, F. and Muhunthan, B., 2009. Effect of cement treatment on geotechnical properties of some Washington State soils. *Engineering geology*, 104(1–2), pp.119–125.

Tripura, D.D., Gupta, S., Debbarma, B. and Deep, R.S.S., 2020. Flexural strength and failure trend of bamboo and coir reinforced cement stabilized rammed earth wallettes. *Construction and Building Materials*, 242, p.117986.

Tsuchida, T. and Tang, Y.X., 2015. Estimation of compressive strength of cement-treated marine clays with different initial water contents. *Soils and Foundations*, 55(2), pp.359–374.

Wang, Z., Liu, T., Long, Z., Wang, J. and Zhang, J., 2023. Predicting the drift capacity of precast concrete columns using explainable machine learning approach. *Engineering Structures*, 282, p.115771.

Zhao, Z., Duan, W., Cai, G., Wu, M. and Liu, S., 2022. CPT-based fully probabilistic seismic liquefaction potential assessment to reduce uncertainty: Integrating XGBoost algorithm with Bayesian theorem. *Computers and Geotechnics*, 149, p.104868.